JOURNAL OF THE ROYAL SOCIETY Interface

rsif.royalsocietypublishing.org

Research

Cite this article: Antoniou Kourounioti RL, Band LR, Fozard JA, Hampstead A, Lovrics A, Moyroud E, Vignolini S, King JR, Jensen OE, Glover BJ. 2013 Buckling as an origin of ordered cuticular patterns in flower petals. J R Soc Interface 10: 20120847.
http://dx.doi.org/10.1098/rsif.2012.0847

Received: 15 October 2012
Accepted: 3 December 2012

Subject Areas:
biomechanics

Keywords:
buckling, cuticle, diffraction grating, elasticity, flower iridescence, nanoridges

Authors for correspondence:
Oliver E. Jensen
e-mail: oliver.jensen@manchester.ac.uk
Beverley J. Glover
e-mail: bjg26@cam.ac.uk

Royal Society Publishing
Informing the science of the future

Buckling as an origin of ordered cuticular patterns in flower petals

Rea L. Antoniou Kourounioti[1], Leah R. Band[2,3], John A. Fozard[2], Anthony Hampstead[1], Anna Lovrics[4], Edwige Moyroud[5], Silvia Vignolini[6], John R. King[2,3], Oliver E. Jensen[2,7] and Beverley J. Glover[5]

[1]Multidisciplinary Centre for Integrative Biology, and [2]Centre for Plant Integrative Biology, School of Biosciences, University of Nottingham, Sutton Bonington LE12 5RD, UK
[3]School of Mathematical Sciences, University of Nottingham, University Park, Nottingham NG7 2RD, UK
[4]Biotalentum Ltd, Szent-Györgyi Albert u 4, Gödöllő 2100, Hungary
[5]Department of Plant Sciences, University of Cambridge, Cambridge CB2 3EA, UK
[6]Cavendish Laboratory, University of Cambridge, J J Thomson Avenue, Cambridge CB3 0HE, UK
[7]School of Mathematics, University of Manchester, Oxford Road, Manchester M13 9PL, UK

The optical properties of plant surfaces are strongly determined by the shape of epidermal cells and by the patterning of the cuticle on top of the cells. Combinations of particular cell shapes with particular nanoscale structures can generate a wide range of optical effects. Perhaps most notably, the development of ordered ridges of cuticle on top of flat petal cells can produce diffraction-grating-like structures. A diffraction grating is one of a number of mechanisms known to produce 'structural colours', which are more intense and pure than chemical colours and can appear iridescent. We explore the concept that mechanical buckling of the cuticle on the petal epidermis might explain the formation of cuticular ridges, using a theoretical model that accounts for the development of compressive stresses in the cuticle arising from competition between anisotropic expansion of epidermal cells and isotropic cuticle production. Model predictions rationalize cuticle patterns, including those with long-range order having the potential to generate iridescence, for a range of different flower species.

1. Introduction

The epidermal surfaces of petals display a range of patterns [1–4]. These patterns result from the combination of diverse micro- and nanostructures, which, together with cell shapes, sculpt the outermost layer of the petal and confer unique physical, mechanical or optical properties on the petal.

In one example, micropapillae and nanofolds on top of the petals of rose provide superhydrophobicity and a high adhesive force with water, a phenomenon known as the 'petal effect'. This effect allows spherical water droplets to form, which cannot roll off even when the petal is turned upside down [5]. Many other petals possess conical cells covered with a radiate pattern of cuticular ridges [1], which might provide functional support for the cell. Finally, arrays of regularly spaced nanoridges have been found on the flat epidermis of *Hibiscus trionum* and many species of tulip, where they act as a diffraction grating. The particular shape and spacing of these ridges cause constructive interference for different wavelengths of light in different directions, giving rise to an angular colour variation, also known as iridescence [6]. Very little is currently known of how any of these patterns form on top of the epidermis during petal development.

Explaining how the nanoscale ridges of a diffraction grating (examples are shown in figure 1*b*,*e*) form on top of the petals is particularly important because of their biological function. Pollinators, such as bumblebees, can detect the iridescent signal produced by petal nanoridges, and can learn to use this signal as a cue to identify rewarding flowers [6]. Understanding how petals develop structures such as these to attract their pollinators is a major

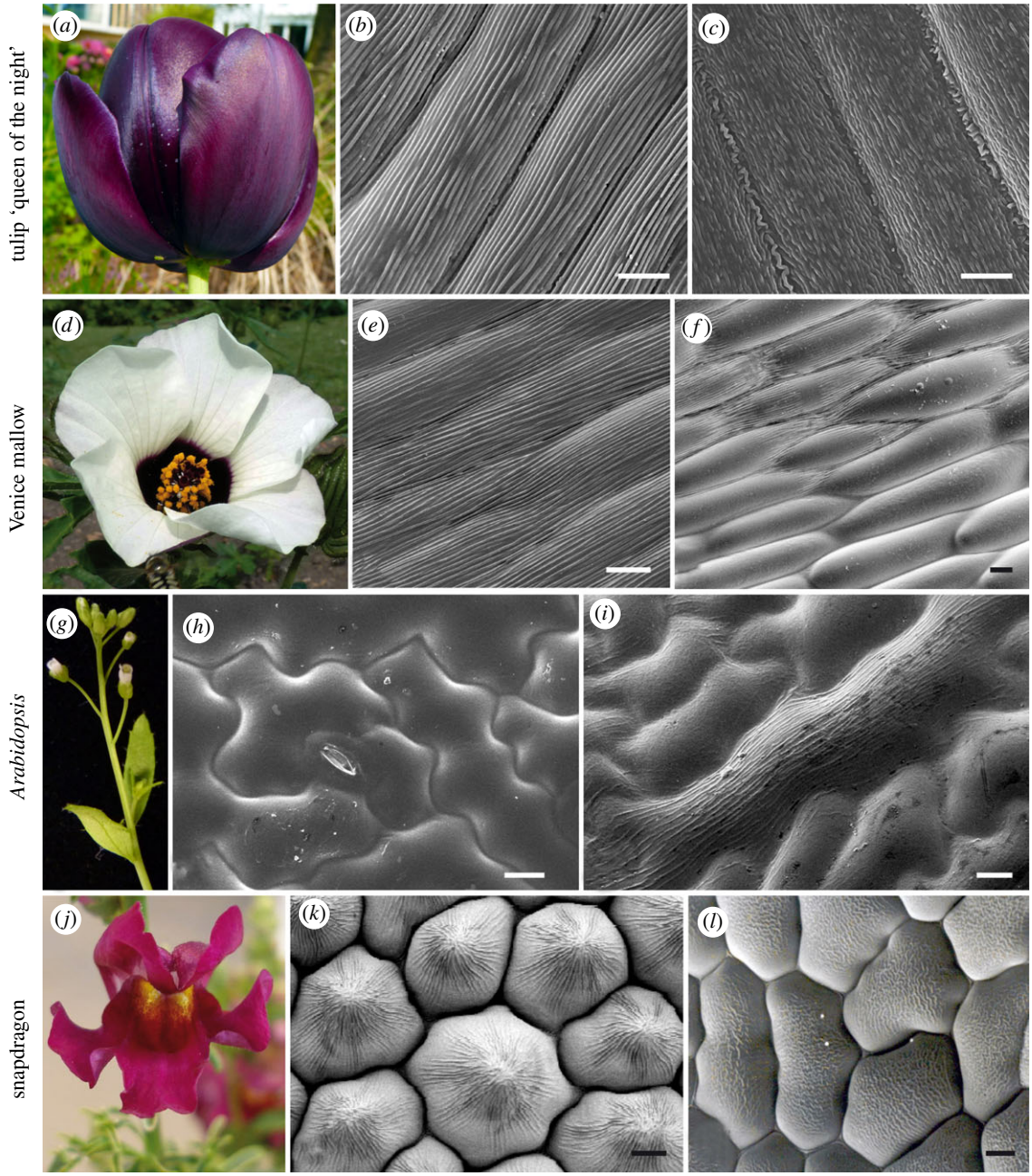

Figure 1. Diversity of surface patterning in flowering plants. Flowers of tulip 'queen of the night' (*a*) produce iridescence owing to the presence of ridges (*b*) on top of the purple-pigmented abaxial (outer) epidermis of the tepal. The adaxial (inner) side of the tepal produces disordered ridges (*c*) and is not iridescent. The dark pigmented patch in the centre of the Venice mallow (*Hibiscus trionum*) flower (*d*) is also iridescent and exhibits flat cells with regular ridges (*e*). At the junction between the purple patch and the rest of the petal (white region), the cells retain their shape and size but the ridges are absent (*f*). Epidermal cells of *Arabidopsis* (*Arabidopsis thaliana*) leaves (*g*) are flat and smooth (*h*) in wild-type individuals but ridges form (*i*) when the *SHINE1* gene, normally silent in leaves, is ectopically expressed (*35S::AtSHN1*) [7]. The inner petal epidermis of wild-type snapdragon (*j*) flowers (*Antirrhinum majus*) is made of conical cells (*k*). These cells remain flat when the *MIXTA* gene, which normally triggers the formation of conical cells, is mutated (*l*) [8]. (*b*,*c*,*e*,*f*,*h*,*i*,*k* and *l*) Scanning electron microscope images; scale bars, 10 µm. (Online version in colour.)

goal in plant biology: an estimated 35 per cent of global crop production depends on petal-mediated animal pollination but a decrease in pollinator numbers across the world has started to limit the odds of pollination and to reduce crop production rates [9,10]. Defining the mechanisms that underlie the development of diffraction gratings, and other petal surface patterns, will allow us to understand how plants can build structures sufficiently regular to mediate interspecies communication through light interference. Since many signalling pathways and morphogenic processes are broadly conserved in biology, understanding how petal surface patterns develop may also have broader implications in understanding many aspects of biological pattern formation.

The optical properties of a petal strongly depend on the shape of its epidermal cells and on the form of the nanoscale patterning on those epidermal cells. To generate iridescence through a diffraction grating, cells must be flat. In contrast, rounded or conical cells scatter light in different directions. The genetic basis of gross epidermal cell shape is well understood, being controlled by a family of MYB transcription factors encoded by the *MIXTA-like* genes [8,11,12]. The nanoscale ridges on many petals, including those that function as diffraction gratings, are part of the cuticle, the

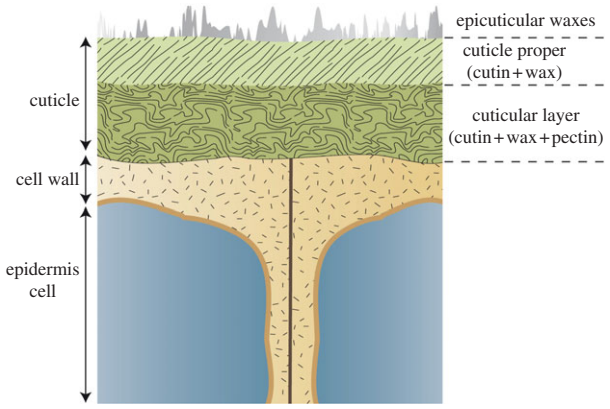

Figure 2. Organization of the plant cuticle. Epidermal cells produce the cuticle, a polymer matrix known to contain cutin, waxes and sometimes polysaccharides (pectin) of the cell wall. In addition, wax crystals are sometimes present on top of the cuticle proper. These basic components can be organized differently to create a smooth or a patterned surface (see figures 1 and 3 for examples), which forms a boundary between the plant and its environment. (Online version in colour.)

protective waxy covering produced by the epidermal cells. Our understanding of the mechanisms that regulate the assembly and organization of the cuticle is still limited. The cuticle consists of a polymer matrix of cutin that is covered with epicuticular waxes and incorporates intracuticular waxes (figure 2). Its thickness, structure and chemical composition vary widely between species and between different organs of the same plant, but the potential functional consequences of such differences are poorly understood [13]. The synthesis of cuticular components (mostly cutin and waxes) and their secretion through the plasma membrane have been described [14–16], and regulators of cutin and wax biosynthetic genes have been recently identified as *SHINE* transcription factors, members of the AP2 family [7,17,18]. However, the mechanisms responsible for the patterning of the cuticle remain to be understood.

Cuticular ridges can be parallel to (figure 1*b*,*e*) or perpendicular to (figure 3*b*,*d*) the long axis of the cell, or can lie in a more complex pattern; some examples are summarized in table 1. It is possible that different mechanisms generate these different patterns [19], or that their control is through the same or similar processes. One possibility is that patterning is controlled by a biochemical process intrinsic to the cuticle (for instance, cuticle components could self-organize). A second possibility is that the cell locally regulates the secretion or assembly of cuticle components in a patterned fashion along the plasma membrane. Alternatively, the ridges could simply form through a mechanical instability, owing to forces arising within the expanding cuticle layer as the cell elongates. (It is notable that mechanical buckling has been proposed as a possible mechanism for the formation of a diffraction grating on a pollinator, namely the cuticle of scales on the wings of *Colias eurytheme* butterflies [20].)

We explore here a biomechanical mechanism for ridge formation, using a mathematical model to demonstrate the underlying principles. The literature on buckling instabilities of thin layers of material on a substrate provides us with a useful starting point. Experimentally, it is well established that lateral compression can be used to manipulate buckling patterns [21]. Orthogonal compressive and extensional stresses will generate organized wrinkled patterns. These are susceptible to secondary instabilities (such as herringbone patterns) if the stress field becomes compressive in both directions [22]. Fig. 8 of Audoly & Boudaoud [23] provides a schematic map of parameter space identifying stability boundaries for the onset of different patterns in a composite layer (a stiff film bound to a soft substrate) under biaxial compression, a framework that we adopt below. In these examples, compressive stresses can arise either through external compression or through swelling or growth of a material such as a gel. An investigation of a growing soft layer on a stiff substrate [24] predicted that the wavelength of the most unstable mode at the onset of instability was infinitely small. This effect was shown to be regularized by the introduction of small inhomogeneity near the surface of the layer, and, in a number of such cases, the wavelength of the mode which first becomes unstable scales with the layer thickness.

In this study, we develop a biomechanical model to investigate whether buckling of the cuticle layer can create the ridge patterns observed on petals and leaves. In §2, we investigate the stresses within the cuticle layer, showing how compressive stresses may arise as a result of differences between the rate of cuticle production and the growth of the underlying cell wall, paying attention to competition between isotropic deposition of cuticle and anisotropic cell expansion. The model predicts how parameters relating to cell expansion, cell shape and cuticle production rate can affect the ridge pattern. Having analysed the origin of the ridges, we return to our list of observed patterns (table 1) in §3. We discuss how these observations can be captured by the model in given parameter regimes, with corroboration provided by the cuticular patterns observed in lines misexpressing the *SHINE* and *MIXTA* genes. Owing to the difficulty in measuring the mechanical properties of the cuticle, we concentrate on qualitative differences in the types of patterns generated. We conclude by discussing the experimentally verifiable predictions provided by the model of how cell growth rates and cuticle production vary between different species and developmental stages.

2. Material and methods

2.1. Modelling buckling patterns in flat cells

We examine how differences between the (anisotropic) growth of the cell wall and the production of cuticle (assumed to be transversely isotropic) generate stresses in the cuticle layer. We explore the concept that compressive stresses can lead to mechanical instabilities that generate ridges in the cuticle.

The cuticle has been shown to be viscoelastic and strain-hardening, with biomechanical properties that depend strongly on temperature and humidity, and having distinct molecular components that regulate different mechanical properties [25,26]. However, to explore and illustrate the underlying mechanism generating ridges, we use here a deliberately simple model, treating the cuticle as a homogeneous incompressible nonlinearly elastic material. The aim of this analysis is to understand how the stresses in the cuticle layer depend upon the growth rates of the cell wall and cuticle. As our primary concern is to determine whether these stresses are compressive or tensile, the precise choice of constitutive law is of secondary importance.

We first consider rectangular cells with a flat upper surface upon which lies a cuboidal layer of cuticle material. The cuticle has uniform principal stretches (λ_1, λ_2, λ_3) in a Cartesian coordinate system (figure 4), with λ_1 and λ_2 in the plane of the cuticle layer, parallel and perpendicular to the long axis of the cell, respectively; incompressibility requires that the stretch normal

Table 1. List of the different cuticular patterns considered in this study. The pattern column shows a representative sketch of the appearance of the cell surface (cf. images in figure 1 or references); cases 1–3 are elongated rectangular cells, cases 4–6 are approximately circular or hexagonal cells and cases 7 and 8 are irregular leaf epidermal cells.

case	pattern	plant species	genotype	position	cell shape	references
1	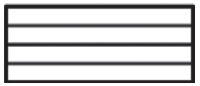	(a) Venice mallow	wild type	base of the petal	flat	figure 1*e*
		(b) tulip	wild type	outer surface of tepal	flat	figure 1*b*
2		Venice mallow	wild type	junction between the purple and white regions of the petal	flat	figure 1*f*
3	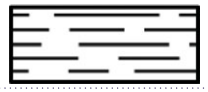	tulip	wild type	inner surface of tepal	flat	figure 1*c*
4		(a) *Arabidopsis*	wild type	petal (adaxial)	conical	[18]
		(b) snapdragon	wild type	inner petal lobe	conical	figure 1*k*
5	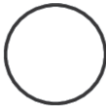	*Arabidopsis*	35S:*miR-SHN1/2/3*	petal (adaxial)	conical	[18]
6		snapdragon	*MIXTA* mutant	inner petal lobe	flat	figure 1*l*
7	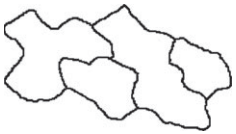	*Arabidopsis*	wild type	leaf (adaxial)	flat	figure 1*h*
8	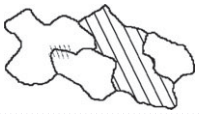	*Arabidopsis*	35S::*SHN1*	leaf (adaxial)	flat	figure 1*i*

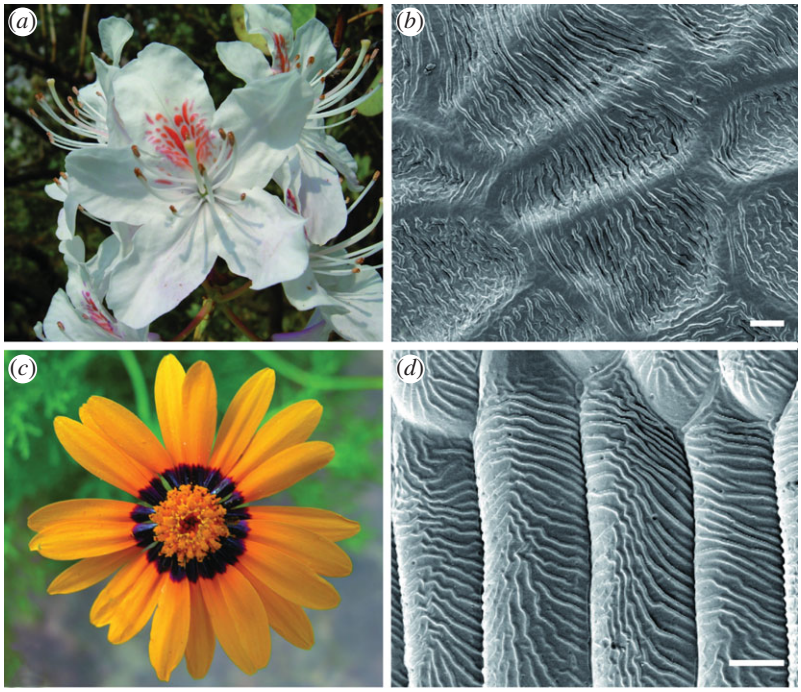

Figure 3. Examples of perpendicular ridges. The epidermal cells of the petals of Yunnan rhododendron (*a,b*) (*Rhododendron yunnanense*) and the daisy *Ursinia calendulifolia* (*c,d*) are striated but the ridges form perpendicularly to the axis of elongation of the cells (compare with figure 1*b,e*). (*b,d*) Scanning electron microscope images; scale bars, 10 μm. (Online version in colour.)

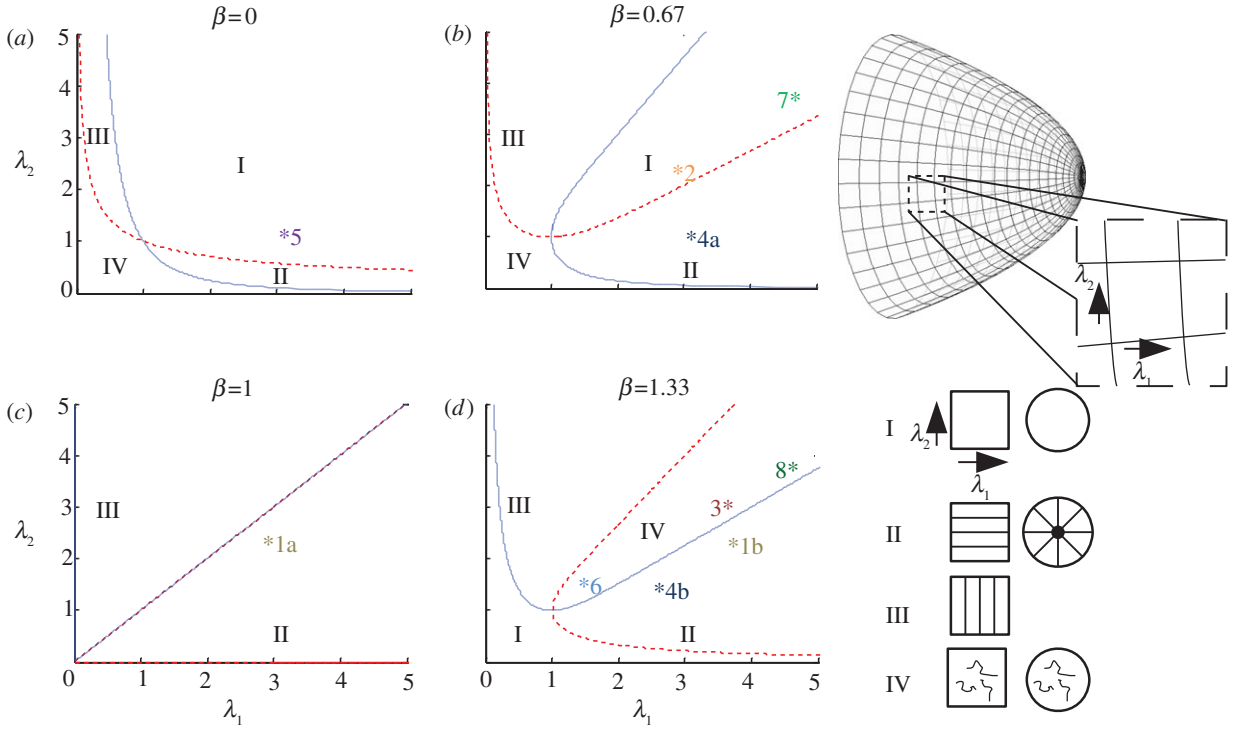

Figure 4. Model predictions of cuticle ridge patterns. (*a–d*) The dependence of the predicted patterns on λ_1 and λ_2, which are the stretches parallel and perpendicular to the long axis for rectangular cells, and in the radial and azimuthal directions for conical or domed cells, for a number of different values of the cuticle production rate β ($\beta < 1$ corresponds to under-production; $\beta > 1$ to over-production; the case $\beta = 0$ is representative of cases in which the growth-induced stress Π (see (2.4) is weak relative to elastic stress in the cuticle layer). Regions I–IV are demarcated using (2.5) (along the solid line $\sigma_{11} = 0$ and along the dashed line $\sigma_{22} = 0$), and correspond to patterns of the type illustrated in the right-hand diagram (for rectangular and circular cells). Asterisks in (*a–d*) mark representative parameter values for each of the different cases considered in table 1: 1a, Venice mallow; 1b, tulip; 2, Venice mallow; 3, tulip; 4a, *Arabidopsis*; 4b, snapdragon; 5, *Arabidopsis* 35S:*miR-SHN1/2/3*; 6, snapdragon *MIXTA*; 7, *Arabidopsis* leaf wt; 8, *Arabidopsis* leaf 35S::*SHN1*. (Online version in colour.)

to the cuticle satisfies $\lambda_3 = 1/\lambda_1\lambda_2$. We assume that the cuticle adheres tightly to the underlying cell wall, and that this is much stiffer than the cuticle, so that λ_1 and λ_2 are prescribed by the growth of the cell wall over the duration of cuticle development. (For flat cells, these stretches will reflect cell growth; stretches can also be generated by the cells becoming domed, as discussed below.) Stretching will cause the cuticle layer to thin, and we suppose that new material is added from the base to maintain a roughly constant cuticle thickness. We suppose, for simplicity, that the new cuticle material is laid down with the same strain as the existing material, so that λ_1 and λ_2 can be assumed homogeneous through the cuticle layer.

We use a neo-Hookean constitutive law to model the relationship between stress and strain in the layer. This is one of the simplest possible nonlinear elastic constitutive laws, with only one material parameter, and it extends Hooke's Law to non-infinitesimal strains. The non-zero stresses in the layer are given by

$$\sigma_{11} = \mu\lambda_1^2 - p, \quad \sigma_{22} = \mu\lambda_2^2 - p \quad \text{and} \quad \sigma_{33} = \frac{\mu}{\lambda_1^2\lambda_2^2} - p, \tag{2.1}$$

in Cartesian coordinates (e.g. [27]; eqn (5.4.2)), where μ is the shear modulus of the cuticle and the pressure p is introduced to enforce incompressibility. As the stresses are uniform and homogeneous, the equilibrium condition $\nabla \cdot \sigma = 0$ is automatically satisfied. We postulate that, as part of the growth response, an additional compressive stress $\mu\Pi$ is applied to the upper and lower surfaces of the cuticle layer (where Π is a stretch-dependent quantity, defined below); one candidate mechanism contributing to Π may be cutin polymerization, which has recently been demonstrated to take place extracellularly by the acyltransferase CD1 [28]. This stress acts through the boundary condition $\sigma_{33} = -\mu\Pi$, and so we require

$$p = \frac{\mu}{\lambda_1^2\lambda_2^2} + \mu\Pi, \tag{2.2}$$

giving

$$\sigma_{11} = \mu\left(\lambda_1^2 - \frac{1}{\lambda_1^2\lambda_2^2}\right) - \mu\Pi \tag{2.3a}$$

and

$$\sigma_{22} = \mu\left(\lambda_2^2 - \frac{1}{\lambda_1^2\lambda_2^2}\right) - \mu\Pi. \tag{2.3b}$$

When $\Pi > 0$, this growth-induced compressive stress (acting normal to the cell wall) effectively adds to the pressure in the cuticle, relieving the tension generated through stretching. A similar approach has been adopted within a linear elasticity framework by Edwards & Schwarz [29], who directly introduced an isotropic stress to a two-dimensional model of a planar cell layer to represent cellular contractility.

To model the additional compressive stress, we postulate

$$\Pi = \beta\left(\lambda_1\lambda_2 - \frac{1}{\lambda_1^2\lambda_2^2}\right). \tag{2.4}$$

This functional form is motivated by the observation that, when the cell wall expands isotropically ($\lambda_1 = \lambda_2$) with $\beta = 1$, the value of Π exactly balances the stresses in the cuticle plane generated by stretching, so that the expanding cuticle is stress-free. We therefore regard the case $\beta = 1$ as that of 'normal' cuticle production. We refer to the cases $\beta > 1$ and $\beta < 1$ as 'over-production' and 'under-production', respectively (although, in this simple model, we do not distinguish explicitly between, for example, the rate of delivery of material to the cuticle layer and its subsequent polymerization). When $\beta > 1$, extra compressive in-plane stress is generated in the cuticle layer, whereas $\beta < 1$ leads to greater tensile in-plane stress in the cuticle. In (2.4), the compressive stress Π depends symmetrically on λ_1 and λ_2, implying that the cuticle growth response is transversely isotropic. Substituting (2.4) into (2.3), we have

$$\frac{\sigma_{11}}{\mu} = \lambda_1(\lambda_1 - \beta\lambda_2) + \frac{\beta - 1}{\lambda_1^2\lambda_2^2} \tag{2.5a}$$

and

$$\frac{\sigma_{22}}{\mu} = \lambda_2(\lambda_2 - \beta\lambda_1) + \frac{\beta - 1}{\lambda_1^2\lambda_2^2}. \tag{2.5b}$$

Using these formulae, we can map out regions of the (λ_1, λ_2)-plane (figure 4) in which the following stress patterns arise:

Region I. $\sigma_{11} > 0$, $\sigma_{22} > 0$: the cuticle layer is under tension in both in-plane directions, suggesting the cuticle will be smooth.

Region II. $\sigma_{11} > 0$, $\sigma_{22} < 0$: the cuticle layer is under tension in the 1 direction, but compression in the 2 direction, so the cuticle will buckle for sufficiently great compressive stresses, forming ridges aligned with the 1 direction.

Region III. $\sigma_{11} < 0$, $\sigma_{22} > 0$: the cuticle layer is under tension in the 2 direction, compression in the 1 direction. Again, for sufficiently great compressive stresses, the cuticle will buckle, forming ridges aligned with the 2 direction.

Region IV. $\sigma_{11} < 0$, $\sigma_{22} < 0$: the cuticle layer is under compression in both in-plane directions, which if sufficiently large will promote buckling with irregular patterns that may not show a preferred orientation.

In general, according to (2.5), the cuticle is completely stress-free only at $\lambda_1 = \lambda_2 = 1$ (no cell growth), except when $\beta = 1$, in which case the cuticle is stress-free along the line $\lambda_1 = \lambda_2$ (isotropic cell growth). We emphasize that the present model does not include viscous processes that might lead to slow stress relaxation in the cuticle layer. Since we do not expect cell shrinkage, we focus on the regime $\lambda_1 \geq \lambda_2 \geq 1$ in the following discussion; however, for completeness, we show the domain $\lambda_1 \geq 0$, $\lambda_2 \geq 0$ in figure 4.

For $0 \leq \beta < 1$, the cuticle is predicted to be smooth if λ_1 and λ_2 are of similar size (region I in figure 4*a*,*b*), whereas ridges are predicted if one stretch is sufficiently large with the other remaining small. We emphasize that patterns with a high degree of spatial correlation are most likely to arise when the cuticle is compressed in one direction and under tension in the other (regions II and III in figure 4).

For $\beta > 1$, cuticle over-production promotes buckling for any $\lambda_1 \geq 1$ and $\lambda_2 \geq 1$ provided that λ_1 and λ_2 are not both unity. As β becomes large, the region in (λ_1, λ_2)-space for which the cuticle is under compression in only one of the two directions becomes smaller, and instead the cuticle is typically compressed in both directions (region IV in figure 4*d*), which we expect to result in irregular buckling patterns. A variety of different patterns are possible in region IV [23], including the ordered ones present in II and III; however, in regions II and III only ordered patterns are expected.

For $\beta = 1$, the cuticle is compressed in the direction of lower stretch and under tension in the direction of greater stretch, so ridges are generated only parallel to the direction of greatest stretch (regions II and III in figure 4*c*). Note that these patterns are predicted to occur even with small anisotropy in the growth rates of the underlying cell.

2.2. Modelling buckling patterns in domed cells

This analysis can be extended to address the case of cells that are not flat, provided that the thickness of the cuticle is small compared with the radii of curvature of the surface, with λ_1 and λ_2 again being the in-plane principal stretches of the cuticle (in orthogonal directions). We illustrate this by considering the case of a cell with a conical upper surface undergoing uniform meridional stretch λ_1. As shown in appendix A, the azimuthal stretch λ_2 is given by

$$\lambda_2 = \lambda_1 \cos\phi, \tag{2.6}$$

where ϕ is the angle between the unit normal to the surface and the axis of symmetry of the cone (so the opening angle of the cone is $\pi - 2\phi$). We can combine (2.6) with (2.5) to predict the principal in-plane stresses in the cuticle. For a growing conical cell, the stretches follow the path (2.6) in the (λ_1, λ_2)-plane. Consider for example the case of cuticle under-production ($0 < \beta < 1$, figure 4*b*). For a flat enlarging cell ($\phi = 0$, $\lambda_1 = \lambda_2$), stretches satisfying (2.6) lie in region I, implying that the cuticle will be smooth. For a sufficiently pointed cell ($\cos\phi < \beta$ for large λ_1), stretches satisfying (2.6) lie in region II, implying that the cuticle will be wrinkled with ridges radiating outwards. Such a mechanism shows parallels with experiments by Huang *et al.* [30], which show that indentation of a plane elastic film generates a radial

wrinkling pattern. In the case of cuticle over-production, sufficiently flat cells ($\cos\phi > 1/\beta$ for large λ_1) are predicted to show irregular patterns (region IV, figure 4*d*), while more conical cells will again show radial ridges (region II).

2.3. Analysing the buckling wavelength

The above calculations show how the production rate of the cuticle, the (anisotropic) growth of the underlying cell wall and possibly the cell shape may lead to stress patterns in the cuticle that induce buckling patterns, and how these patterns may be strongly correlated over long distances under appropriate circumstances. For buckling patterns to be iridescent, the distance between ridges must be regular and comparable in magnitude to the wavelength of light. From microscopic images of ridges, we observe that their wavelength appears to be similar to the thickness of the cuticle, of the order of 1 μm. The following two observations demonstrate how the physical properties of the cuticle layer (figure 2) might be regulated to ensure that the buckling wavelength is comparable to the cuticle layer depth.

First, consider the buckling under lateral compression of a thin elastic film of thickness h and Young's modulus E_f bonded to an incompressible elastic substrate of thickness H and Young's modulus E_s. (We can identify the upper film with the cutin + wax layer in figure 2, and the substrate with the thicker cutin + wax + pectin layer.) A balance between the energy of bending of the film and the elastic restoring force of the substrate yields the following predictions for the buckling wavelength γ [31,32]: for a sufficiently soft film ($E_f/E_s \ll (H/h)^3$), the buckling wavelength is short compared with the substrate depth ($\gamma \sim h(E_f/E_s)^{1/3} \ll H$); for a very stiff film ($E_f/E_s \gg (H/h)^3$), the buckling wavelength is long compared with the substrate depth ($\gamma \sim (hH)^{1/2}(E_f/E_s)^{1/6} \gg H$). However, by tuning the relative stiffnesses of the two layers to the relative depths according to

$$\frac{E_f}{E_s} \sim \left(\frac{H}{h}\right)^3, \tag{2.7}$$

the buckling wavelength will be comparable to the substrate depth.

Alternatively, consider a single homogeneous elastic layer resting on a rigid surface, where swelling of the layer leads to buckling. While the critical wavelength for buckling is predicted to be zero for a strictly homogeneous layer [24], a small surface inhomogeneity (e.g. a thin 'skin') is sufficient to make the critical wavelength comparable to the layer thickness. Thus, using either (2.7) or suitable surface modification, the observed ridge wavelengths can be plausibly justified via a buckling mechanism.

3. Results

We now consider the observed nanoridge patterns (classified into eight cases in table 1), and discuss how the model can provide understanding of each of these. We have assigned positions on the graphs in figure 4 for most of the observed cases. These positions do not contain quantitative information but are shown as candidate explanations for the observed data, focusing on the regions in which the points lie and the positions relative both to each other and to the line $\lambda_1 = \lambda_2$.

3.1. Buckling can explain the ridge patterns in rectangular cells

Ridges parallel to the principal elongation axis are observed in rectangular cells of tulip and Venice mallow (case 1*a*,*b*). In the model, these patterns are predicted in parameter regimes corresponding to region II, where the cuticle is under tension parallel to the long axis of the cell but compressed in the direction perpendicular to it. We illustrate these cases with representative points in figure 4*c*,*d*, but elsewhere in region II would also be valid, depending on the precise growth kinematics of the underlying cell wall.

In contrast with these regular patterns, cells in the middle of the petal of Venice mallow (case 2) do not have ridges, suggesting that the cuticle is under tension in both planar directions. We suggest that this change in morphology is due to the cuticle production rate being lower than that of the cells at the base of the petal (case 1*a*; Venice mallow); in the model this corresponds to a lower value of β, but the same values of λ_1 and λ_2, producing a change from region II to region I. We have selected points in figure 4*c*,*b*, respectively, to illustrate this hypothesis.

Tulip cells on the inside of the petals have ridges which are not continuous (case 3); we suggest that these are due to a parameter set lying in region IV, reflecting biaxial compression in the cuticle layer. One possible difference between this case and that of the striated cells on the outside of the petal (case 1*b*; tulip) is the size of the stretch perpendicular to the long axis of the cell (λ_2); we have chosen two possible points in figure 4*d* to illustrate how a modest change in cell shape can alter the ridge pattern.

3.2. Buckling can explain the ridges in circular cells

The model can also be applied to circular cells. These often become domed or conical, which can be associated with radial ridges that do not cause iridescence (figure 1*k*). Using equation (2.6), we see that increasing the angle ϕ (making the cell more pointed) increases the ratio λ_1/λ_2; we suppose that the cuticle is under tension along the meridional direction, but the slower growth in the azimuthal direction generates compressive forces that cause radial ridges. Such ridges are predicted to correspond to region II, thus we adopt the parameter sets shown in figure 4*b*,*d* for *Arabidopsis* and snapdragon, respectively (case 4*a*,*b*), prior to considering how the patterns may change in misexpression lines.

3.3. Buckling can explain the ridges in *SHINE* and *MIXTA* misexpression lines

The petals of the *Arabidopsis SHINE* amiRNA line [18] have convex circular cells with smooth surfaces (case 5), which we expect to correspond to points in region I. This transgenic line is likely to have reduced cuticle production, which corresponds to a lower value of β, but similar values of stretches λ_1 and λ_2 to the wild type (case 4*a*; *Arabidopsis*) [18]. As with the rectangular cells in Venice mallow (cases 1*a* and 2), decreasing β can cause a transition from region II to region I; we illustrate the effect of silencing *SHINE* genes by choosing a point in region I of figure 4*a* having the same stretches as the wild type (case 4*a*) in figure 4*b*.

Mutation of the *MIXTA* gene in snapdragon changes petal epidermal cells from conical to flat [8]; the ridges become disordered (case 6; figure 1*l*), which our model suggests corresponds to a transition from region II to region IV. From (2.6), reducing the angle ϕ while keeping the azimuthal stretch λ_2 constant decreases the radial stretch λ_1; we therefore choose a point on figure 4*d* (case 6) with the same level of over-production $\beta > 1$ as the wild type (case 4*b*; snapdragon) but a lower value of λ_1.

Observed ridges in *Arabidopsis* leaves also corroborate the model predictions (cases 7 and 8; figure 1*g*,*h*). Wild-type leaves (case 7) are smooth (region I, figure 4*b*), but the

transgenic *Arabidopsis* line overexpressing *SHINE* (case 8) has disordered ridges (region IV, figure 4*d*), and it is thought that there is over-production of cuticle [17]. The complex shapes of *Arabidopsis* leaf cells make it difficult to estimate λ_1 and λ_2; however, we choose a point in region I of figure 4*b* to illustrate the wild-type case and a point in region IV of figure 4*d* for the mutant, with the same stretches λ_1 and λ_2 but an increased production rate β.

4. Discussion

We have used a simple mathematical model to illustrate a possible biomechanical mechanism for the formation of ridges in the cuticle on the surface of epidermal cells of plant petals and leaves. The model builds on the concept that the ridge patterns reflect features of the stress field within the cuticle layer. Very regular patterns that are correlated over long distances are likely to arise via compression in the direction orthogonal to ridges and tension parallel to them. Disordered patterns of ridges are likely to reflect biaxial compression, whereas a smooth cuticle is likely instead to be under biaxial tension. We assume that these stresses arise from expansion of the underlying cell and deposition of the cuticle layer as the cell expands. In the absence of detailed information on how new cuticle material is integrated into the existing cuticle layer, we have postulated a parsimonious constitutive model for the mechanical properties of the cuticle, assuming that it is incompressible, nonlinearly elastic and subject to a growth-induced stress arising from deposition and polymerization of new material. The growth-induced stress Π (see equation (2.4)) is chosen to ensure that the cuticle can remain stress-free when the underlying cell wall expands isotropically; Π is also assumed to be transversely isotropic, implying that cuticle production is not biased by the orientation (in structure or expansion rate) of the underlying cell wall.

The mathematical model illustrates how ridge patterns may be altered by changes in cell expansion kinematics, or by over- or under-production of cuticle. At a qualitative level, four broad classes of ridge patterns can be generated (regions I–IV, figure 4), with the rates of cuticle production and the principal stretches in the plane of the cell surface being the controlling parameters (the latter can be influenced by the topography of the cell surface). To produce an iridescent diffraction grating, cells must be flat and the cuticle ridges on their surface must be very regular (region II) and with suitable spacing; our model suggests that the ridge spacing is determined primarily by cuticle thickness, which may vary depending on the rate of synthesis and export of cuticular component or the polymerization of the cutin itself. Our model is consistent with the reduction in ridge patterns arising in *SHINE* knockdown lines in *Arabidopsis* for which there is reduced cuticle production [7,18], and with observations that intracellular cutin synthesis (by the biosynthetic enzymes GPAT6 and CYP77A6) is essential to the formation of ridges in cuticle of *Arabidopsis* flowers [33]. Also, ridges on top of *Arabidopsis* petal conical cells are absent in the *abcg13* knockout mutant [34]. ABCG13 is an ABC transporter required for the extracellular secretion of cuticular lipids in flowers, suggesting that affecting the transport of cuticle components ultimately modifies the surface pattern. The recent identification of CD1, a cutin synthase localized directly in the cuticle [28], indicates that cutin polymerization influences cuticle thickness and potentially cuticular patterning, as the cuticle becomes much thinner when cutin polymerization is impaired [28]. Our model also provides a reasonable explanation for the altered ridge patterns in the snapdragon *MIXTA* mutant, for which there is a change in cell shape and hence in the cuticle stress distribution.

There are numerous areas where more detailed studies of cuticle properties are warranted. In our model, we have taken no account of possible viscous relaxation of stresses generated in the cuticle, nor of the age structure through the cuticle layer, nor of the precise nature of cross-linking within the cuticle layer that might generate the hypothesized stress Π (although the identification of CD1 as an extracellular cutin synthase [28] provides a promising lead). It will be important to develop more detailed microstructural models as more detailed knowledge of cuticle properties becomes available. It would also be of interest in future studies to track the evolving shape of individual petal cells and map the changes in principal stretches with time, tracking out a path through (λ_1, λ_2)-space in figure 4, to see when cuticle patterns emerge as the cell expands. Future work should also address how ridge formation is coordinated between neighbouring cells, allowing ridges to be uninterrupted at the junction between two consecutive cells in some cases (figure 1*e*), while allowing discontinuous patterns at the junction between striated and non-striated cells in other instances (figure 1*f*,*i*).

In addition to the examples of ridge patterns discussed earlier (table 1), ridges that are perpendicular to the long axis of the cell have been observed on the flowers of species of rhododendron and daisies (figure 3). According to our model, such patterns suggest that the cuticle is compressed along the long axis of the cell and under tension perpendicular to it (region III in figure 4, for which $\lambda_2 > \lambda_1$). If cuticle production is initiated when such cells have aspect ratio of roughly unity, and if the cells subsequently elongate while remaining flat, then necessarily $\lambda_1 > \lambda_2$, and region III is inaccessible. However, if cuticle production starts at a different phase in the expansion of the cell then it may be possible for the cell to expand laterally sufficiently to enter region III. For example, an out-of-plane expansion (generating a humped cross-section) could also allow λ_2 to increase relative to λ_1. The pertinent stretches are those generated over the period when the cuticle develops, which may be different from those over the whole growth of the cell. Such considerations raise interesting questions about the growth history of cells and the timing of cuticle development.

The Centre for Plant Integrative Biology (CPIB) is a centre for integrative systems biology supported by the BBSRC and EPSRC. The research presented here is an outcome of the Fifth Mathematics in the Plant Sciences Study Group, held in Nottingham, UK, in January 2012, and funded by BBSRC and EPSRC via CPIB and GARNet. The authors gratefully acknowledge study group participants for their helpful discussions during the event. Work in B.J.G.'s laboratory on floral iridescence is supported by the Leverhulme Trust. L.R.B. is grateful for funding from the Leverhulme Trust in the form of an Early Career Fellowship.

Appendix A. Principal stretches in an axisymmetric cuticle

Consider cuticle on an axisymmetric cell surface, parametrized by the arc-length s from the axis of symmetry along a meridian, the angle ϕ between the unit normal to the cell

surface and the axis of symmetry and the azimuthal angle θ. The shape of the cell is defined with respect to cylindrical polar coordinates (r,θ, z) by

$$\frac{\mathrm{d}r}{\mathrm{d}s} = \cos\phi \quad \text{and} \quad \frac{\mathrm{d}z}{\mathrm{d}s} = -\sin\phi. \tag{A 1}$$

We take the reference state of the cuticle to be flat ($\phi = 0$), parametrized by arc-length $\tilde{r} = \tilde{s}$, with $\tilde{z} = 0$. Then the principal in-plane stretches in the meridional and azimuthal directions are, respectively [35],

$$\lambda_1 = \frac{\mathrm{d}s}{\mathrm{d}\tilde{s}} \quad \text{and} \quad \lambda_2 = \frac{r}{\tilde{s}}. \tag{A 2}$$

For a cone with uniform ϕ, it follows from (A 1) that $r = s\cos\phi$. Assuming uniform meridional stretch, so that $s = \lambda_1\tilde{s}$, (A 2) then yields (2.6).

References

1. Kay QON, Daoud HS, Stirton CH. 1981 Pigment distribution, light reflection and cell structure in petals. *Bot. J. Linnean Soc.* **83**, 57–84. (doi:10.1111/j.1095-8339.1981.tb00129.x)
2. Baagoe J. 1977 *Microcharacters in the ligules of the compositae*. London, NY: Academic Press.
3. Baagoe J. 1978 Taxonomical application of ligule microcharacters in compositae, 2. Arctotideae, Asteraceae, Calenduleae, Eremothamneae, Inuleae, Liabeae, Mutisieae, and Senecioneae. *Bot. Tidsskr.* **72**, 125–147.
4. Stirton CH. 1980 *Petal sculpturing*. London, UK: HMSO.
5. Feng L, Zhang Y, Xi J, Zhu Y, Wang N, Xia F, Jiang L. 2008 Petal effect, a superhydrophobic state with high adhesive force. *Langmuir* **24**, 4114–4119. (doi:10.1021/la703821h)
6. Whitney HM, Kolle M, Andrew P, Chittka L, Steiner U, Glover BJ. 2009 Floral iridescence, produced by diffractive optics, acts as a cue for animal pollinators. *Science* **323**, 130–133. (doi:10.1126/science.1166256)
7. Aharoni A, Dixita S, Jetterb R, Thoenesa E, van Arkela G, Pereira A. 2004 The SHINE clade of AP2 domain transcription factors activates wax biosynthesis, alters cuticle properties, and confers drought tolerance when overexpressed in *Arabidopsis*. *Plant Cell* **16**, 2463–2480. (doi:10.1105/tpc.104.022897)
8. Noda K, Glover BJ, Linstead P, Martin C. 1994 Flower colour intensity depends on specialized cell shape controlled by a MYB-related transcription factor. *Nature* **369**, 661–664. (doi:10.1038/369661a0)
9. Basu P, Bhattacharya R, Ianetta P. 2011 A decline in pollinator dependent vegetable crop productivity in India indicates pollination limitation and consequent agro-economic crises. *Nat. Precedings*. See http://hdl.handle.net/10101/npre.2011.6044.1.
10. Klein AM, Vaissiere BE, Cane JH, Steffan-Dewenter I, Cunningham SA, Kremen C, Tscharntke T. 2007 Importance of pollinators in changing landscapes for world crops. *Proc. R. Soc. B* **274**, 303–313. (doi:10.1098/rspb.2006.3721)
11. Perez-Rodriguez M, Jaffe F, Butelli E, Glover BJ, Martin C. 2005 Development of three different cell types is associated with the activity of a specific MYB transcription factor in the ventral petal of *Antirrhinum majus*. *Development* **132**, 359–370. (doi:10.1242/dev.01584)
12. Baumann K, Perez-Rodriguez M, Bradley D, Venail J, Bailey P, Jin H, Koes R, Roberts K, Martin C. 2007 Control of cell and petal morphogenesis by R2R3 MYB transcription factors. *Development* **134**, 1691–1701. (doi:10.1242/dev.02836)
13. Riederer M, Müller C. (eds) 2006 *Biology of the plant cuticle*, ch. 1. Annual Plant Reviews, vol. 23. Oxford, UK: Blackwell.
14. Kunst L, Samuels L. 2009 Plant cuticles shine, advances in wax biosynthesis and export. *Curr. Opin. Plant Biol.* **12**, 721–727. (doi:10.1016/j.pbi.2009.09.009)
15. Samuels L, Kunst L, Jetter R. 2008 Sealing plant surfaces, cuticular wax formation by epidermal cells. *Annu. Rev. Plant Biol.* **59**, 683–707. (doi:10.1146/annurev.arplant.59.103006.093219)
16. Pollard M, Beisson F, Li Y, Ohlrogge JB. 2008 Building lipid barriers, biosynthesis of cutin and suberin. *Trends Plant Sci.* **13**, 236–246. (doi:10.1016/j.tplants.2008.03.003)
17. Broun P, Poindexter P, Osborne E, Jiang C-Z, Riechmann JL. 2004 WIN1, a transcriptional activator of epidermal wax accumulation in *Arabidopsis*. *Proc Natl Acad. Sci. USA* **101**, 4706–4711. (doi:10.1073/pnas.0305574101)
18. Shi JX, Malitsky S, De Oliveira S, Branigan C, Franke RB, Schreiber L, Aharoni A. 2001 Shine transcription factors act redundantly to pattern the archetypal surface of *Arabidopsis* flower organs. *PLoS Genetics* **7**, e1001388. (doi:10.1371/journal.pgen.1001388)
19. Koch K, Bohn HF, Barthlott W. 2009 Hierarchically sculptured plant surfaces and superhydrophobicity. *Langmuir* **25**, 14 116–14 120. (doi:10.1021/la9017322)
20. Ghiradella H. 1974 Development of ultraviolet-reflecting butterfly scales, how to make an interference filter. *J. Morph.* **142**, 395–410. (doi:10.1002/jmor.1051420404)
21. Ohzono T, Shimomura M. 2004 Ordering of microwrinkle patterns by compressive strain. *Phys. Rev. B* **69**, 132202. (doi:10.1103/PhysRevB.69.132202)
22. Hutchinson JW, Chen X. 2004 Herringbone buckling patterns of compressed thin films on compliant substrates. *J. Appl. Mech.* **71**, 597–603. (doi:10.1115/1.1751186)
23. Audoly B, Boudaoud A. 2008 Buckling of a stiff film bound to a compliant substrate. Part I. Formulation, linear stability of cylindrical patterns, secondary bifurcations. *J. Mech. Phys. Solids* **56**, 2401–2421. (doi:10.1016/j.jmps.2008.03.003)
24. Ben Amar M, Ciarletta P. 2010 Swelling instability of surface-attached gels as a model of soft tissue growth under geometric constraints. *J. Mech. Phys. Solids* **58**, 935–954. (doi:10.1016/j.jmps.2010.05.002)
25. López-Casado G, Matas AJ, Domínguez E, Cuartero J, Heredia A. 2007 Biomechanics of isolated tomato (*Solanum lycopersicum* l.) fruit cuticles, the role of the cutin matrix and polysaccharides. *J. Exp. Bot.* **58**, 3875–3883. (doi:10.1093/jxb/erm233)
26. Domínguez E, Cuartero J, Heredia A. 2011 An overview on plant cuticle biomechanics. *Plant Sci.* **181**, 77–84. (doi:10.1016/j.plantsci.2011.04.016)
27. Howell PD, Kozyreff G, Ockendon JR. 2009 *Applied solid mechanics*. Cambridge, UK: Cambridge University Press.
28. Yeats TH *et al*. 2012 The identification of cutin synthase, formation of the plant polyester cutin. *Nat. Chem. Biol.* **8**, 609–611. (doi:10.1038/nchembio.960)
29. Edwards CM, Schwarz US. 2011 Force localization in contracting cell layers. *Phys. Rev. Lett.* **107**, 128101. (doi:10.1103/PhysRevLett.107.128101)
30. Huang J, Juszkiewicz M, de Jeu WH, Cerda E, Emrick T, Menon N, Russell TP. 2007 Capillary wrinkling of floating thin polymer films. *Science* **317**, 650–653. (doi:10.1126/science.1144616)
31. Cerda E, Mahadevan L. 2003 Geometry and physics of wrinkling. *Phys. Rev. Lett.* **90**, 074302. (doi:10.1103/PhysRevLett.90.074302)
32. Chung JY, Nolte AJ, Stafford CM. 2011 Surface wrinkling, a versatile platform for measuring thin-film properties. *Adv. Mat.* **23**, 349–368. (doi:10.1002/adma.201001759)
33. Li-Beisson Y, Pollard M, Sauveplane V, Pinot F, Ohlrogge J, Beisson F. 2009 Nanoridges that characterize the surface morphology of flowers require the synthesis of cutin polyester. *Proc. Natl Acad. Sci. USA* **106**, 22 008–22 013. (doi:10.1073/pnas.0909090106)
34. Panikashvili D, Shi JX, Schreiber L, Aharoni A. 2011 The *Arabidopsis* ABCG13 transporter is required for flower cuticle secretion and patterning of the petal epidermis. *New Phytol.* **190**, 113–124. (doi:10.1111/j.1469-8137.2010.03608.x)
35. Preston SP, Jensen OE, Richardson G. 2007 Buckling of an axisymmetric vesicle under compression, the effects of resistance to shear. *Q. J. Mech. Appl. Math.* **61**, 1–24. (doi:10.1093/qjmam/hbm021)